Electronic Supplementary Information (ESI) for

Dendrite-suppressed and utilization-improved metallic Li anode enabled by lithiophilic nano-Pb decoration on carbon cloth

Peng Du,[a] Chenbo Yuan,[a] Xiaoyu Cui,[b] Kaifu Zhang,[a] Yu Yu,[a] Xiaodi Ren,[c] Xiaowen Zhan,*[a,b] and Shan Gao*[a]

[a]*School of Chemistry and Chemical Engineering, Anhui Province Key Laboratory of Chemistry for Inorganic/Organic Hybrid Functionalized Materials, Key Laboratory of Structure and Functional Regulation of Hybrid Materials of Ministry of Education, Anhui University, 230601 Hefei, Anhui, P.R. China*

Email: xiaowen.zhan@ahu.edu.cn (X.Z.); shangao@ahu.edu.cn (S.G.)

[b]*School of Materials Science and Engineering, Anhui University, 230601 Hefei, Anhui, P.R. China*

[c]*Department of Materials Science and Engineering, University of Science & Technology of China, 230026 Hefei, Anhui, P.R. China.*

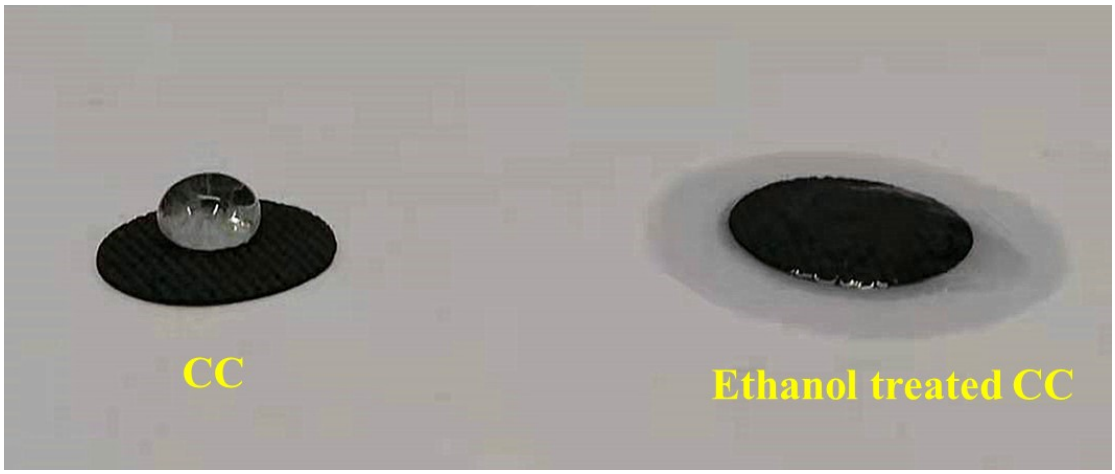

Figure S1. The wetting behavior of aqueous $Pb(Ac)_2 \cdot 3H_2O$ solution on carbon cloth with (left) and without (right) alcohol pre-treatment.

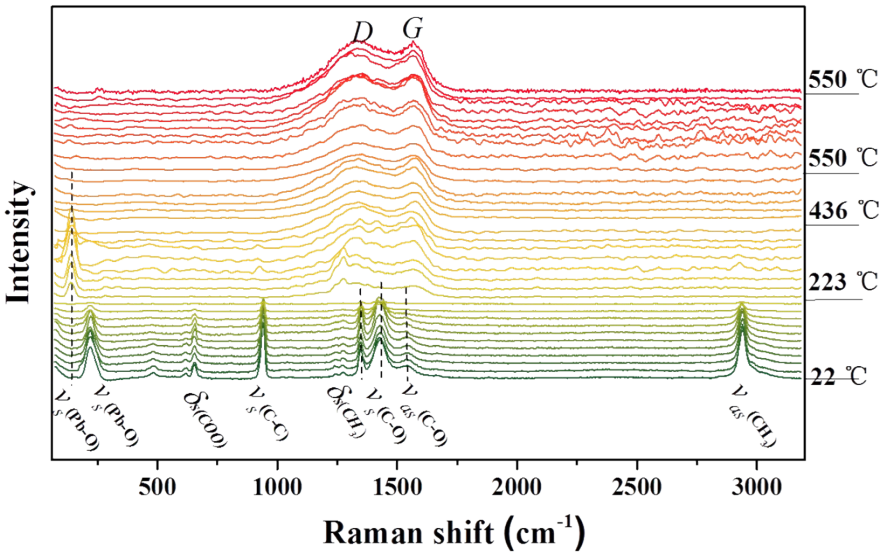

Figure S2. *In-situ* Raman spectra for the heat treatment of $Pb(Ac)_2 \cdot 3H_2O$.

Table S1. Peak assignments for Raman spectra of $Pb(Ac)_2{\cdot}3H_2O$.

Raman shift(cm^{-1})	Vibration name	Vibration mode
1328.78	D-bond	Amorphous carbon
1578.14	G-bond	Graphitized carbon
143.88	V_s (**Pb-O**)	Pb-O stretch
216.93	V_s (**Pb-O**)	Pb-O stretch
657.15	δ_s (**COO**)	COO symmetric deformation
940.27	V_s (**C-C**)	C-C symmetric stretch
1351.35	δ_s (**CH_3**)	CH_3 symmetric deformation
1424.86	V_s (**C-O**)	C-O symmetric stretch; C-O
1539.21	V_{as} (**C-C**)	C-O anti-symmetric stretch; C=O
2940.81	V_{as} (**CH_3**)	CH_3 symmetric stretch

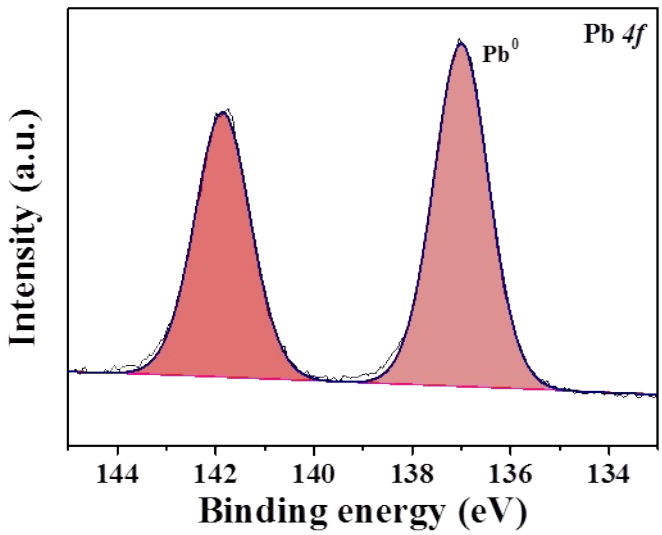

Figure S3. XPS Pb 4f spectrum of Pb@CC.

Table S2. The mass values of different samples under specified conditions during the Pb@CC fabrication process.

Sample conditions	Sample 1	Sample 2	Sample 3	Sample 4	Average values
Prisitne CCs (m0)	27.1 mg	26.8 mg	26.9 mg	26.5 mg	26.8±0.22 mg
CCs after 550 °C calcination (m1)	21.8 mg	21.6 mg	21.9 mg	21.4 mg	21.7±0.19 mg
CCs after $Pb(Ac)_2{\cdot}3H_2O$ (aq.) immersion and 40 °C drying (m2)	31.7 mg	30.5 mg	31.2 mg	31.2 mg	31.2±0.43 mg
Pb@CCs after 550 °C calcination (m3)	25.2 mg	24.7 mg	24.8 mg	24.6 mg	24.8±0.23 mg

Note S1:

After immersion in $Pb(Ac)_2{\cdot}3H_2O$ solution and drying, the average mass loading of $Pb(Ac)_2{\cdot}3H_2O$ on CCs is:

$$\mathbf{m(Pb(Ac)_2{\cdot}3H_2O) = m2\text{-}m0 = 31.2\ mg\text{-}26.8\ mg = 4.4mg.}$$

After final calcination, the average Pb/C loading is:

$$\mathbf{m(Pb+C) = m3\text{-}m1 = 24.8\ mg\text{-}21.7\ mg = 3.1mg.}$$

Assuming all $Pb(Ac)_2{\cdot}3H_2O$ decomposed into Pb and C, then the average Pb loading is:

$$\mathbf{m(Pb) = 4.4\ mg * 207.2\ g\ mol^{-1} / 391.2\ g\ mol^{-1} = 2.3\ mg,}$$

The average C mass is then estimated to be about:

$$\mathbf{3.1\text{-}2.3 = 0.8\ mg.}$$

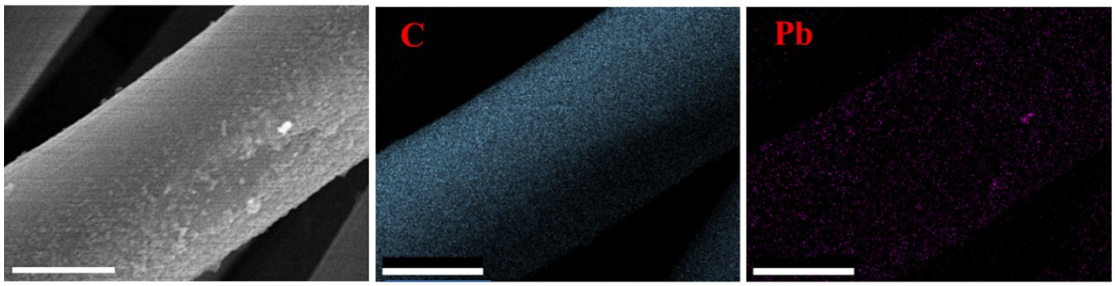

Figure S4. SEM images and EDX maps of the as-prepared Pb@CC. Scale bars: 5 μm.

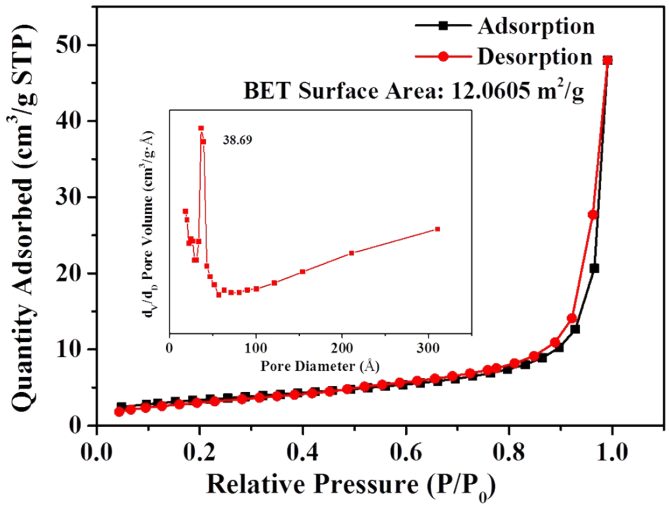

Figure S5. The nitrogen adsorption and desorption isotherms of Pb@CC (inset: pore-size distribution curve).

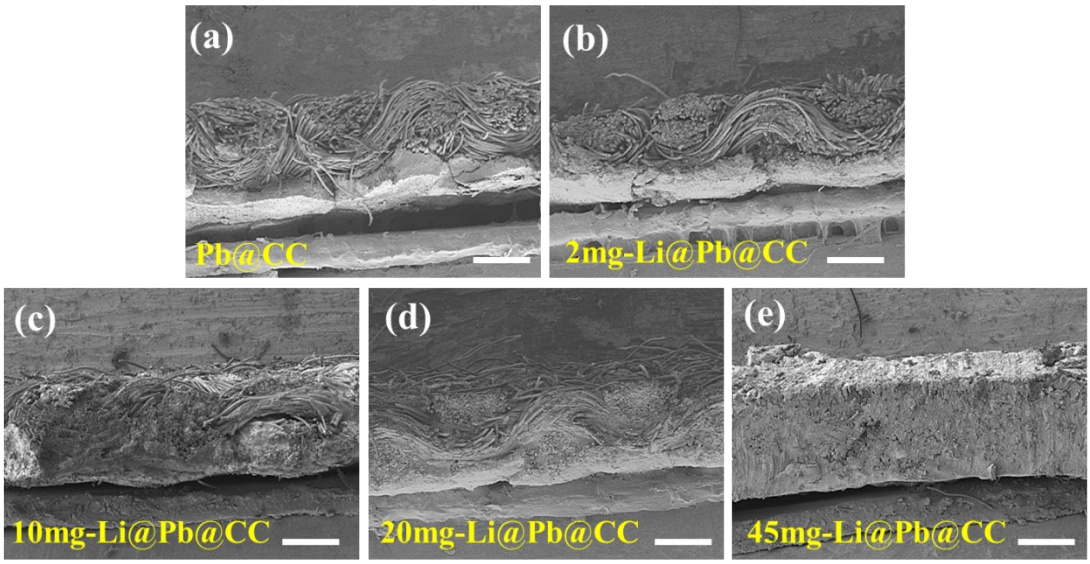

Figure S6. Cross-sectional SEM images of (**a**) Pb@CC, (**b**) 2mg-Li@Pb@CC, (**c**) 10mg-Li@Pb@CC, (**d**) 20mg-Li@Pb@CC and (**e**) 45mg-Li@Pb@CC. Scale bars: 200 µm.

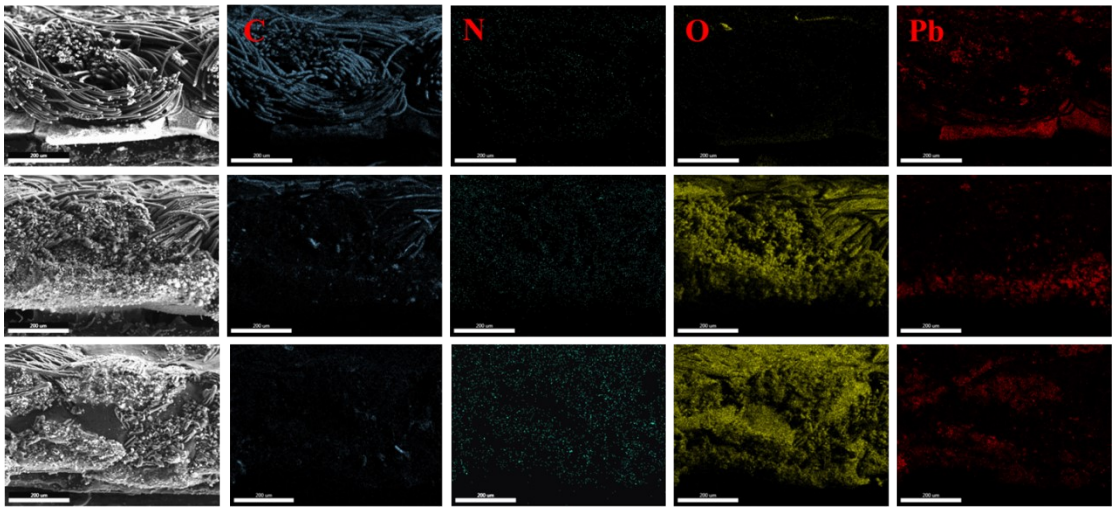

Figure S7. Cross-sectional EDS maps (**a**) Pb@CC, (**b**) 10mg-Li@Pb@CC and (**c**) 45mg-Li@Pb@CC. Scale bars: 200 μm.

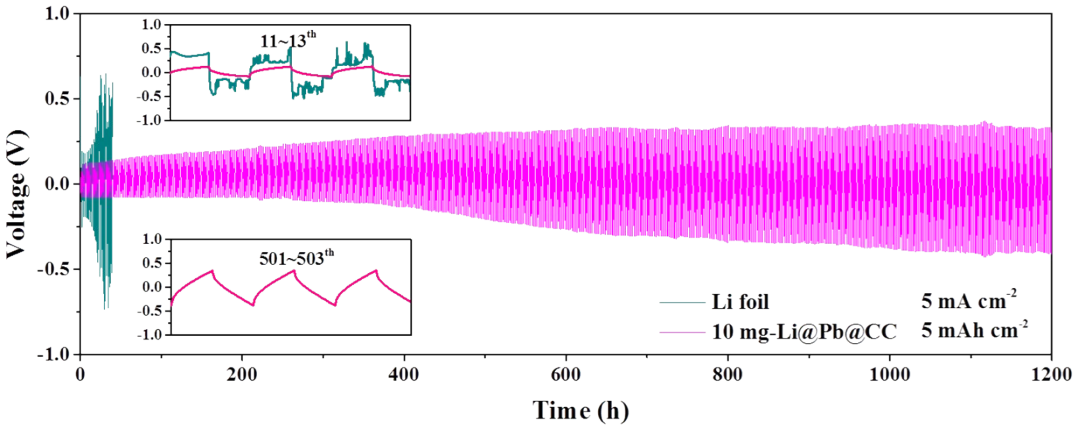

Figure S8. Cycling performance of the Li symmetric cells assembled with Li foils and 10mg-Li@Pb@CC electrodes acquired at 5 mA cm^{-2}.

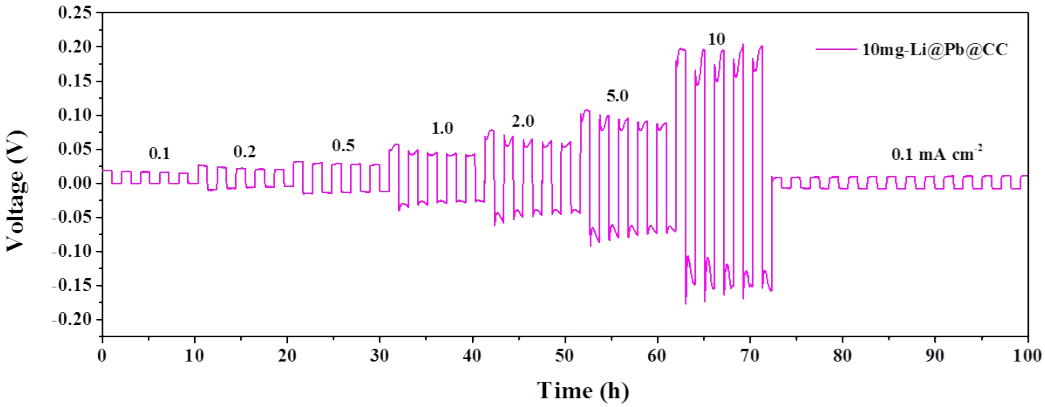

Figure S9. Rate performance of the Li symmetric cells assembled with 10mg-Li@Pb@CC electrodes. The duration was set at 1 h for each plating or stripping process.

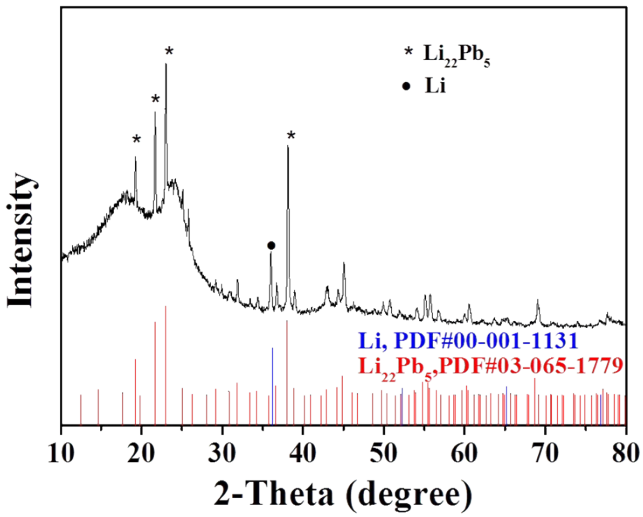

Figure S10. The XRD pattern of 10mg-Li@Pb@CC.

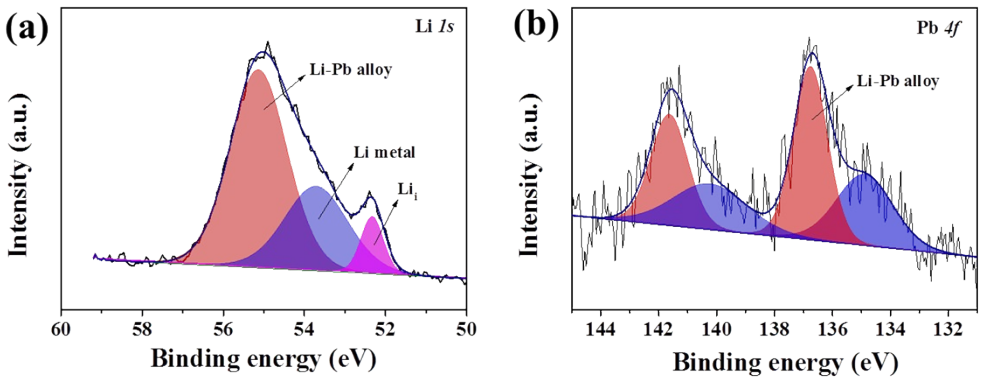

Figure S11. The XPS spectra of 10mg-Li@Pb@CC: (h) Li1s and (i) Pb4f.

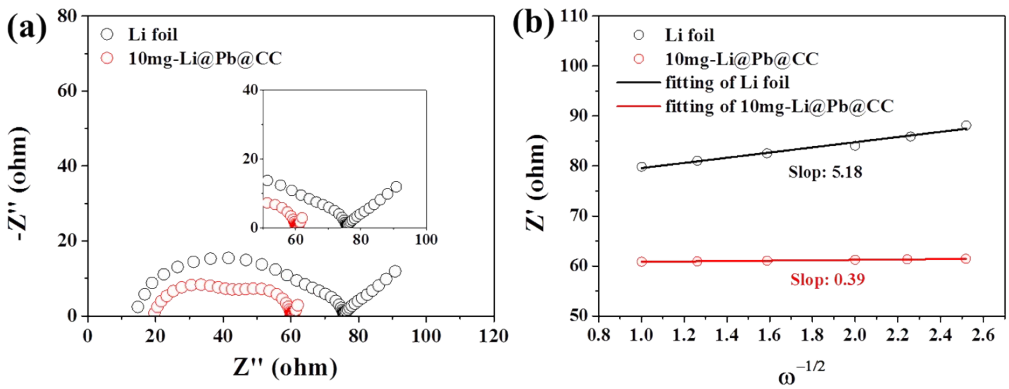

Figure S12. (a) EIS spectra of Li symmetric cells assembled with Li foil and 10mg-Li@Pb@CC electrodes. (b) The plots and fitting results for Z' and $\omega^{-1/2}$ extracted from the corresponding EIS data in the low-frequency regions.

Note S2: The diffusion coefficient of Li (D_{Li}) is calculated based on Eq. (1):

$$D=R_2T_2/2A^2n^4F^4C^2\sigma^2 \quad \text{..... (1)}$$

where R represents the gas constant, T the absolute temperature, A the specific surface area of the electrode, n the number of electron transfer in the redox process, F the Faraday constant, C the Li concentration, and σ the Warburg coefficient. The calculation results are as follows:

$$C_{(Li\,foil)} = \frac{m}{MV_{(Li\,foil)}} = \frac{0.065}{6.94 \times 0.8^2 \times 3.14 \times 0.06} = 0.077\ mol\ cm^{-3}$$

$$D_{(Li\,foil)} = \frac{R^2T^2}{2A^2n^4F^4C^2\sigma^2} = \frac{8.3142^2 \times 298^2}{2 \times 2.0096^2 \times 1^4 \times 96500^4 \times 0.077^2 \times 5.18^2} = 5.51 \times 10^{-14}\ cm^2\ s^{-1}$$

$$C_{(10mg-Li@Pb@CC)} = \frac{m}{MV_{(10mg-Li@Pb@CC)}} = \frac{0.010}{6.94 \times 0.6^2 \times 3.14 \times 0.04} = 0.033\ mol\ cm^{-3}$$

$$D_{(10mg-Li@Pb@CC)} = \frac{R^2T^2}{2A^2n^4F^4C^2\sigma^2} = \frac{8.3142^2 \times 298^2}{2 \times 1.1309^2 \times 1^4 \times 96500^4 \times 0.033^2 \times 0.39^2} = 1.67 \times 10^{-10}\ cm^2\ s^{-1}$$

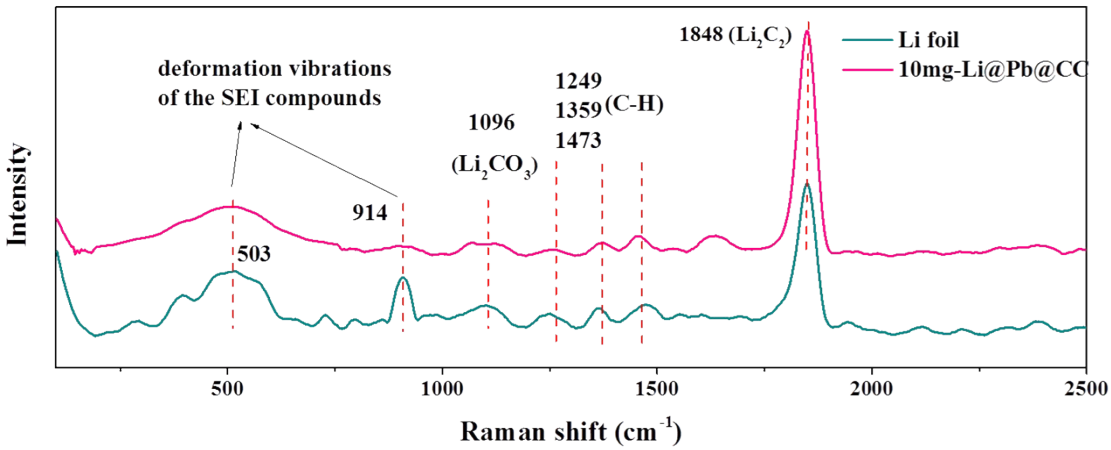

Figure S13. Raman spectra analyzing the solid electrolyte interphase (SEI) of Li foil and 10mg-Li@Pb@CC electrodes after 50 cycles at 1 mA cm^{-2}.

Note S3: The Raman band at 1094 cm^{-1} belongs to Li_2CO_3.[1-3] Li_2CO_3 is one of the main inorganic SEI components. In addition, there are three signals at about 1249, 1375 and 1473 cm^{-1}, which may be related to different C-H vibration modes.[4] Some of them indicate that olefin fragments (another common component of SEI) may have be generated.[5] They also match the stretching $V_{p=O}$ mode of organic phosphorus compounds, such as $(CH_3)_2{}^{-}P(=O)CH_3$, $P(=O)F_3$ and PO_3^{2-}[6] Organic phosphates and derivative compounds are typical decomposition products as $LiPF_6$ can be decomposed to form POF_3, which then evolves into organic phosphate and organic fluorophosphate products. Another strong vibration peak is clearly seen at 1848 cm^{-1}, which points clearly to Li_2C_2.[7] Finally, the peaks at 503 cm^{-1} and 914 cm^{-1} can be assigned to deformation vibrations of the SEI compounds.[8]

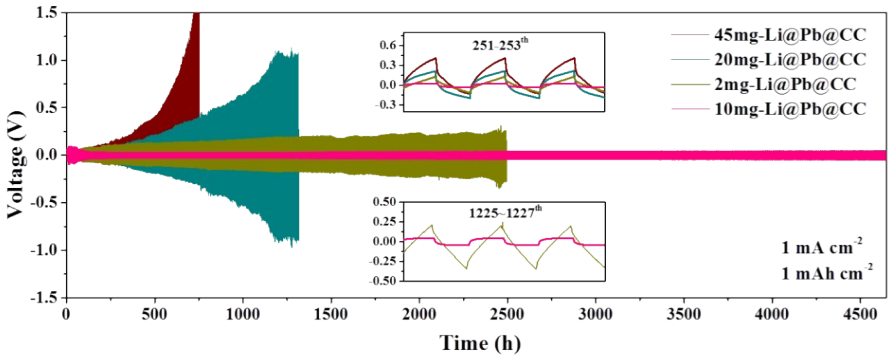

Figure S14. Cycling performance of the Li symmetric cells assembled with 2mg-Li@Pb@CC 10mg-Li@Pb@CC, 20mg-Li@Pb@CC and 45mg-Li@Pb@CC electrodes acquired at 1 mA cm^{-2}.

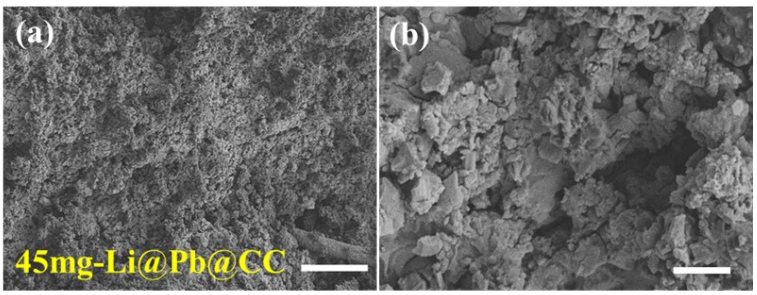

Figure S15. SEM images of the 45mg-Li@Pb@CC electrodes after 50 cycles at 1 mA cm^{-2}/1 mAh cm^{-2}. Scale bars: 50 µm for panel a and 2 µm for panel b.

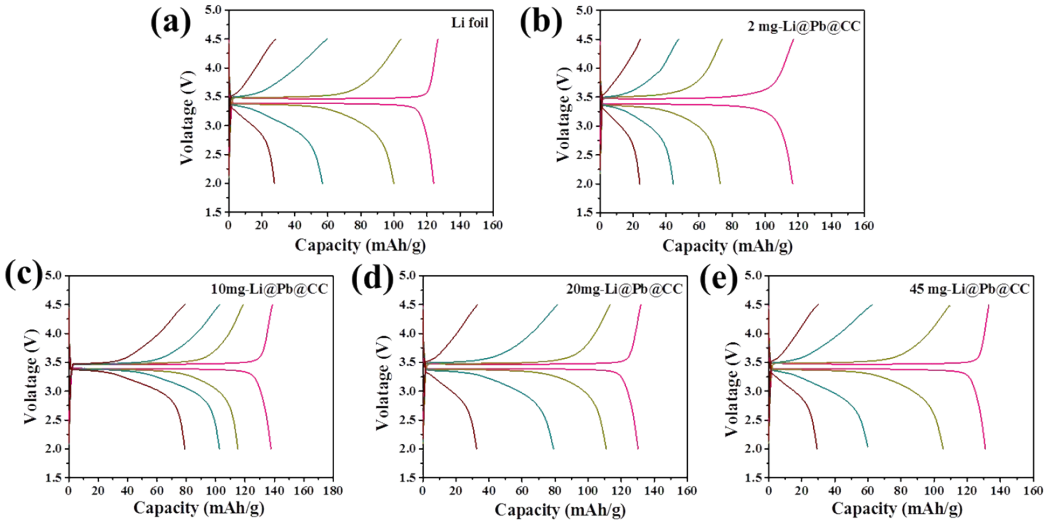

Figure S16. Voltage profiles for the 1st, 200th, 400th and 600th cycles of LFP-based full cells at 1 C with various Li loadings (N/P ratios): (**a**) Li foil, (**b**) 2mg-Li@Pb@CC, (**c**) 10mg-Li@Pb@CC, (**d**) 20mg-Li@Pb@CC and (**e**) 45mg-Li@Pb@CC.

Table S3. Comparison in overpotential and cycle life of our 10mg-Li@Pb@CC electrodes with some representative Li anodes modified by various processing strategies from the literature. The testing conditions are 1 mA cm^{-2} and 1 mAh cm^{-2}.

Material	Electrolyte	Cycle stability	Overpotential	Refs.
Li-C	1 M $LiPF_6$ in (EC/EMC, 3:7 wt %) with 2.0% VC	500 h	46 mV	[9]

Polished Li	1 M $LiPF_6$ in EC:DEC (1:1 vol %)	570 h	48 mV	[10]
LMC-Li	1 M $LiPF_6$ in EC:DMC (1:1 vol %)	1200 h	12 mV	[11]
Housed Li	1.0 M $LiPF_6$ in FEC:DMC (1:1 vol %) with 1.1 wt % $LiNO_3$	950 h	25 mV	[12]
Li-cMOFs	1M $LiPF_6$ in EC/DMC/EMC (1:1:1 vol %)	700 h	29 mV	[13]
Li-Ni@NiO-400	1 M $LiPF_6$ in EC/DMC/EMC (1:1:1 vol %)	2000 h	13 mV	[14]
LCC Composite	1 M $LiPF_6$ in EC/DEC (1:1 vol %).	400 h	10 mV	[15]
C/SiNW/Li	1M $LiPF_6$ in EC/DEC (1:1 vol %).	600 h	100 mV	[16]
CFC/Li	1 M $LiPF_6$ in EC/DEC (1:1 vol %).	400 h	75 mV	[17]
Li/C-ALD	1 M $LiPF_6$ in EC/DEC (1:1 vol %).	800h	~50 mV	[18]
Li-$Ti_3C_2T_x$-rGO	1 M $LiPF_6$ in EC/DMC/EMC (1:1:1 vol %)	1400 h	26 mV	[19]
10mg-Li@Pb@CC	1 M $LiPF_6$ in EC/EMC (3:7 vol %)	4648 h	50 mV	

Table S4. Comparison in full-cell performance and infusion time/temperature of 10mg-Li@Pb@CC electrodes with those from some representative reports in the literature.

N/P	Cathode	Anode	Cycle performance	Infusion time	Infusion temperature	Refs.
291.9~ 324.36	1.19 mAh cm^{-2}, LFP	347.4~385.9 mAh cm^{-2}, AC@CNT/Li	1 C, 92.4 mAh/g after 300 cycles 76.8%.	40 min	300 ℃	[20]

20.2~25.9	0.595~0.765 mAh cm^{-2}, LFP	15.4 mAh cm^{-2}, Li@MgZnO/CNF	5 C, 78.2 mAh/g after 600 cycles 82%	25 s	300 ℃	[21]
24.2	0.883 mAh cm^{-2}, LFP	21.4 mAh cm^{-2}, CF/Ag-Li	1 C, 86 mAh/g after 500 cycles 62.7%	2 min	300 ℃	[22]
208.8	0.612 mAh cm^{-2}, LFP	127.4 mAh cm^{-2}, Li-Co_3O_4/NF	2 C, 102.4 mAh/g after 500 cycles 80.7%	5 s	350 ℃	[23]
29.5~34.1	0.68 mAh cm^{-2}, LFP	23.2~30.9 mAh cm-2, Li/Mo composite	1 C, 136 mAh/g after 200 cycles 90.7%	4 s	350 ◦C	[24]
56.7	0.51 mAh cm^{-2}, LFP	28.9 mAh cm^{-2}, NPCC-Li	2 C, 120 mAh/g after 600 cycles 86.6%	4 s	315 °C	[25]
192.1	0.663 mAh cm^{-2}, LFP	127.4 mAh cm^{-2}, Li/Ag@Cu	0.5 C, 128 mAh/g after 200 cycles 88.2%	5 s	300 °C	[26]
41.4	1.5 mAh cm^{-2}, LFP	62.1 mAh cm^{-2}, Li-NiO/NF	0.5 C, 160 mAh/g after 100 cycles, >90%	6 s	360 °C	[27]
63.28	0.61 mAh cm^{-2}, LFP	38.6 mAh cm^{-2}, 10mg-Li@Pb@CC	1 C, 91.1 mAh/g after 600 cycles 66.2%	~1 s	250 °C	

References

1. S. Tang, Y. Gu, J. Yi, Z. Zeng, S.-Y. Ding, J.-W. Yan, D.-Y. Wu, B. Ren, Z.-Q. Tian and B.-W. Mao, *Journal of Raman Spectroscopy*, 2016, **47**, 1017-1023.
2. S. Hy, Felix, Y.-H. Chen, J.-y. Liu, J. Rick and B.-J. Hwang, *Journal of Power Sources*, 2014, **256**, 324-328.
3. K. Guo, R. Kumar, X. Xiao, B. W. Sheldon and H. Gao, *Nano Energy*, 2020, **68**, 104257.
4. M. J. Piernas-Munoz, A. Tornheim, S. Trask, Z. Zhang and I. Bloom, *Chem Commun (Camb)*, 2021, **57**, 2253-2256.
5. M. Guo, X. Jin and R. E. White, *Journal of The Electrochemical Society*, 2017, **164**, E3200-E3214.
6. S. Nowak and M. Winter, *Molecules*, 2017, **22**, 403.
7. T. A. Galloway, L. Cabo-Fernandez, I. M. Aldous, F. Braga and L. J. Hardwick, *Faraday Discuss*, 2017, **205**, 469-490.
8. R. Schmitz, R. Ansgar Müller, R. Wilhelm Schmitz, C. Schreiner, M. Kunze, A. Lex-Balducci, S. Passerini and M. Winter, *Journal of Power Sources*, 2013, **233**, 110-114.
9. C. Niu, H. Pan, W. Xu, J. Xiao, J. G. Zhang, L. Luo, C. Wang, D. Mei, J. Meng, X. Wang, Z. Liu, L. Mai and J. Liu, *Nat Nanotechnol*, 2019, **14**, 594-601.
10. W. Tang, X. Yin, Z. Chen, W. Fu, K. P. Loh and G. W. Zheng, *Energy Storage Materials*, 2018, **14**, 289-296.
11. Q. Liu, G. Zhu, R. Li, S. Lou, H. Huo, Y. Ma, J. An, C. Cao, F. Kong, Z. Jiang, M. Lu, Y. Tong, L. Ci, G. Yin and J. Wang, *Energy Storage Materials*, 2021, **41**, 1-7.

12. X. Shen, X. Cheng, P. Shi, J. Huang, X. Zhang, C. Yan, T. Li and Q. Zhang, *Journal of Energy Chemistry*, 2019, **37**, 29-34.
13. M. Zhu, B. Li, S. Li, Z. Du, Y. Gong and S. Yang, *Advanced Energy Materials*, 2018, **8**, 1703505.
14. G. Li, S. Xu, B. Li, T. Xia, J. Yu, F. Shao, Z. Yang, Y. Su, Y. Zhang, J. Ma and N. Hu, *Journal of Power Sources*, 2021, **506**, 230161.
15. R. Zhang, Y. Li, M. Wang, D. Li, J. Zhou, L. Xie, T. Wang, W. Tian, Y. Zhai, H. Gong, M. Gao, K. Liang, P. Chen and B. Kong, *Small*, 2021, **17**, e2101301.
16. P. Zhang, C. Peng, X. Liu, F. Dong, H. Xu, J. Yang and S. Zheng, *ACS Appl Mater Interfaces*, 2019, **11**, 44325-44332.
17. S. Liu, X. Xia, Z. Yao, J. Wu, L. Zhang, S. Deng, C. Zhou, S. Shen, X. Wang and J. Tu, *Small Methods*, 2018, **2**. 1800035.
18. B. Zhao, B. Li, Z. Wang, C. Xu, X. Liu, J. Yi, Y. Jiang, W. Li, Y. Li and J. Zhang, *ACS Appl Mater Interfaces*, 2020, **12**, 19530-19538.
19. Y. Fang, Y. Zhang, K. Zhu, R. Lian, Y. Gao, J. Yin, K. Ye, K. Cheng, J. Yan, G. Wang, Y. Wei and D. Cao, *ACS Nano*, 2019, **13**, 14319-14328.
20. J. Wang, H. Liu, H. Wu, Q. Li, Y. Zhang, S. Fan and J. Wang, *Carbon*, 2021, **177**, 181-188.
21. T. Le, Q. Liang, M. Chen, C. Yang, Z. Yu, J. Cheng, F. Kang and Y. Yang, *Small*, 2020, **16**, e2001992.
22. R. Zhang, X. Chen, X. Shen, X.-Q. Zhang, X.-R. Chen, X.-B. Cheng, C. Yan, C.-Z. Zhao and Q. Zhang, *Joule*, 2018, **2**, 764-777.
23. G. Huang, P. Lou, G.-H. Xu, X. Zhang, J. Liang, H. Liu, C. Liu, S. Tang, Y.-C. Cao and S. Cheng, *Journal of Alloys and Compounds*, 2020, **817**, 152753.
24. J. Zhang, Q. Li, Y. Zeng, Z. Tang, D. Sun, D. Huang, Z. Peng, Y. Tang and H. Wang, *Chemical Engineering Journal*, 2021, **426**, 131110.
25. K. Li, Z. Hu, J. Ma, S. Chen, D. Mu and J. Zhang, *Adv Mater*, 2019, **31**, e1902399.
26. L. Wu, W. Jiang, H. Zou, C. Ye, J. Zhang, G. Xu, X. Li, Z. Yue, F. Sun and L. Zhou, *Journal of Materials Chemistry A*, 2021, **9**, 20748-20757.
27. Q. Zhang, W.-L. Bai, C.-Y. Sun, X. Liu, K.-X. Wang and J.-S. Chen, *Chemical Engineer ing Journal*, 2021, **405,** e2001992.